Mixing and Combustion of Turbulent Coaxial Jets
An Application of Computational Fluid Dynamics to Swirling Flows

Teresa Parra[1], Ruben Perez[1], Miguel A. Rodriguez[1], Artur Gutkowski[2], Robert Szasz[3] and Francisco Castro[1]

[1] *Department of Energy and Fluid Mechanics, University of Valladolid, Paseo del Cauce 59, 47011 Valladolid, Spain*
[2] *Department of Heat Technology and Refrigeration, Technical University of Lodz, Lodz, Poland*
[3] *Energy Division, Lund University, Lund, Sweden*

Keywords: CFD, Swirl Number, Recirculation Zones, Burner.

Abstract: The aim of this research is gaining an insight into flow patterns in swirling burners. These are suitable for lean mixtures, because of procuring the fix position of the flame. The interaction of the two reactive confined swirling jets leads to the formation of complex patterns which are not well understood. In the present study, these flow patterns are numerically investigated using Reynolds Averaging Navier-Stokes (RANS) equations for the flow and a Probability Density Function is used for modelling the combustion. Two swirl numbers were characterised: 0.14 and 0.74. Strong swirling annular jets are responsible of an inner recirculation zone. Low swirling flows produce poorer mixture and wide flame fronts whereas strong swirling flows are precursors of mixing enhancement and thing flame fronts.

1 INTRODUCTION

The paper is focused on studying the flow pattern of the flame for low and high swirl number. Swirling flows let burn lean mixtures near the flammability limits and produce low emissions.

The simplest burners are based on the interaction of two confined coaxial jets. Annular jet goes through a swirler that gives azimuthal component to the flow. The exit of the two coaxial nozzles to the chamber with an expansion ratio of four in area produces the separation of the annular boundary layer. The swirling annular jet is responsible for the radial pressure gradient. For swirl numbers over 0.6, there is reverse flow in the centre of the chamber.

The benchmark of Roback and Johnson (Roback, 1983) is the set up chosen to study the influence of the swirler. This burner has two coaxial nozzles that discharge into a test chamber. Figure 1 shows and scheme of the burner and table 1 presents a summary of the main dimensions and operation conditions of this test case.

The swirler is a certain number of fixed vanes located in the annular nozzle. The change of the trailing edge angle modifies the Swirl number of the annular jet. This paper is devoted to study the flow pattern of the flame for low and high swirl numbers.

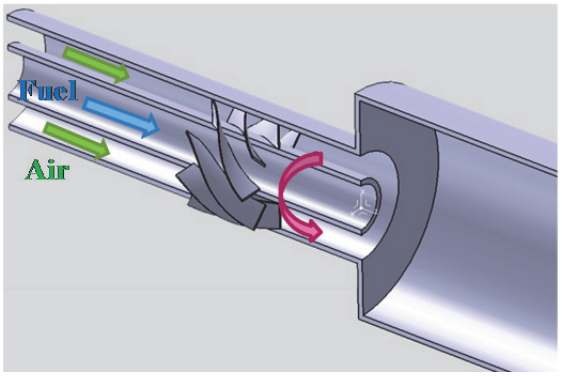

Figure 1: Scheme of the Roback-Johnson swirling burner.

The definition of Swirl number is the ratio of azimuthal momentum and axial momentum. The clear classification of low and high swirl numbers is related to the flow pattern.

Low-swirl injector (S < 0.6) produces in the test chamber a Central Divergence Zone (CDZ), a Shear Layer (SL) and an Outer Recirculation Zone (ORZ). Whereas high-swirl injectors are precursors of an Inner Recirculation Zone (IRZ), a Shear Layer (SL)

Parra T., Perez R., Rodriguez M., Gutkowski A., Szasz R. and Castro F..
Mixing and Combustion of Turbulent Coaxial Jets - An Application of Computational Fluid Dynamics to Swirling Flows.
DOI: 10.5220/0005009005450550
In *Proceedings of the 4th International Conference on Simulation and Modeling Methodologies, Technologies and Applications* (SIMULTECH-2014), pages 545-550
ISBN: 978-989-758-038-3

and an Outer Recirculation Zone (ORZ), (García-Villalba, 2006$_a$; García-Villalba 2006$_b$). See figure 2 for details of the described flow pattern.

Table 1: Dimension details, boundary conditions and fluid properties.

	Fuel	Oxidizer
Injection	Central Nozzle	Annular Nozzle
Nozzles' diameter inner-outer (mm)	0-25	31-59
Composition	CH_4	22% O_2 78% N_2
Temperature (K)	300	900
Velocity (m/s)	0.66	1.54
Turbulence intensity (%)	12	7.5
Specific Heat(J/kg/K)	Polynomial function of temperature	
Thermal Conductivity (W/m/K)	0.0332	0.0242
Viscosity (kg/m/s)	$1.087.10^{-5}$	$1.7894.10^{-5}$
Molecular Weight (kg/kmol)	16.04303	28.996

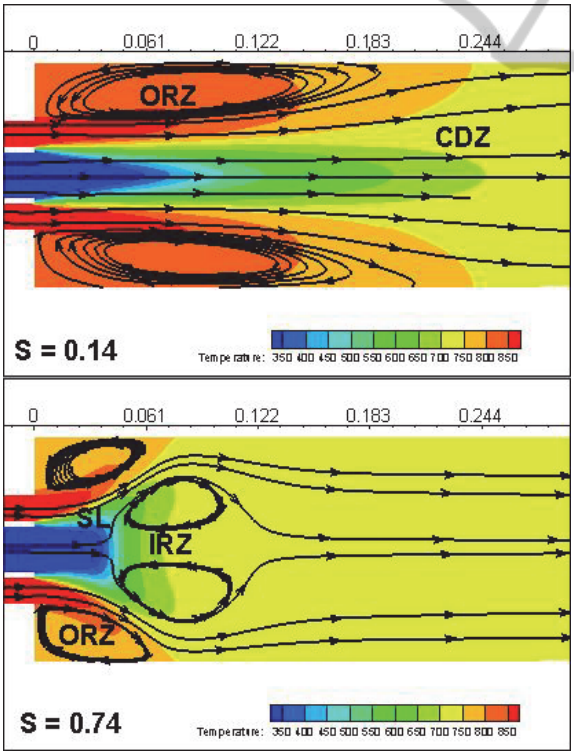

Figure 2: Contours of temperature in the longitudinal plane and stream lines to locate recirculation zones for non reactive cases.

The interest for swirling burners is based on their low emissions and the possibility to burn lean mixtures, (Parra, 2014; Parra 2015).

2 NUMERICAL MODEL

The three dimensional domain has the following spatial resolution: Δ~d/190 in the test chamber, Δ~d/40 in the central nozzle and Δ~d/46 in the annular nozzle, being d the diameter of the chamber, diameter of central nozzle and difference of diameters of the annular nozzle respectively, and Δ the dimension of the cell. To sum up, the computational domain has around 10 million hexahedral cells. The mesh is decomposed to be solved in parallel being the criterion the minimum number of cells in the interface to save computational time associated to information transfer.

Navier-Stokes equations for transient, incompressible, turbulent and reactive flows were solved using Total Variation Diminishing. Pressure-Velocity coupling was PISO. Multigrid resolution improves the performance towards the full convergence.

Anisotropy of the swirling flow makes difficult to model the turbulence. The chosen model was RNG k-ε model dominated by the swirl. Because it considers source term R_ε based on the strain tensor, (Versteeg, 1995). Its conservation equations are described in equations (1) and (2).

$$\frac{\partial}{\partial t}(\rho k) + \frac{\partial}{\partial x_i}(\rho k u_i) = \frac{\partial}{\partial x_j}\left(\alpha_k \mu_{eff} \frac{\partial k}{\partial x_j}\right) + G_k - \rho\varepsilon \quad (1)$$

$$\frac{\partial}{\partial t}(\rho\varepsilon) + \frac{\partial}{\partial x_i}(\rho\varepsilon u_i) = \frac{\partial}{\partial x_j}\left(\alpha_\varepsilon \mu_{eff} \frac{\partial \varepsilon}{\partial x_j}\right) + C_{1\varepsilon}\frac{\varepsilon}{k}G_k - C_{2\varepsilon}\rho\frac{\varepsilon^2}{k} - R_\varepsilon \quad (2)$$

Enhanced wall treatment is used as turbulence treatment near the walls, hence the mesh was generated for $\Delta y^+ = 1$.

2.1 Combustion Model

A suitable approach for turbulent non premixed reacting flows is to use the mixture fraction defined as a function of local mass fraction and their corresponding in the combustible and oxidizer jets.

$$f = \frac{Y_i - Y_{i,o}}{Y_{i,c} - Y_{i,o}} \tag{3}$$

Local thermodynamic properties are predicted from the mixture fraction distribution. Hence the hypothesis of infinite Damköhler number is assumed, that is instantaneous chemical reaction after mixing is achieved, (Kuo, 1986). This method let estimate intermediate species without solving a detailed mechanism of reaction.
The code solves the transport equations for both mixture fractions $\bar{f}$and the variance $\overline{f'^2}$ as proposed by Jones (Jones, 1982):

$$\frac{\partial}{\partial t}(\rho\bar{f}) + \frac{\partial}{\partial x_i}(\rho u_i \bar{f}) = \frac{\partial}{\partial x_i}\left(\frac{\mu_t}{\sigma_t}\frac{\partial}{\partial x_i}\bar{f}\right) \tag{4}$$

$$\frac{\partial}{\partial t}(\rho\overline{f'^2}) + \frac{\partial}{\partial x_i}(\rho u_i \overline{f'^2}) = -C_d\rho\frac{\varepsilon}{k}\overline{f'^2} + \\ + \frac{\partial}{\partial x_i}\left(\frac{\mu_t}{\sigma_t}\frac{\partial}{\partial x_i}\overline{f'^2}\right) + C_g\mu_t\left(\frac{\partial}{\partial x_i}\bar{f}\right)^2 \tag{5}$$

with σ_t, C_g and C_d values equal to 0.7, 2.86 and 2 respectively.

The use of the Probability Density Function (PDF) p(f) converts the time averaged mixture fraction and variance, $\bar{f}$ and $\overline{f'^2}$, into the instantaneous mixture fraction f. The PDF can be calculated assuming equilibrium or measured from experiments. Finally, local temperature and composition are evaluated as equation 6 where $\overline{\emptyset}_i$.represents either temperature or mass fractions.

$$\overline{\emptyset}_i = \int_0^1 p(f)\emptyset_i(f)df \tag{6}$$

Figures 3 and 4 show the sample for temperature and carbon monoxide at different scaled heat loss (HL) or gain (HG) as well as adiabatic flames obtained from experimental data and used for simulations.

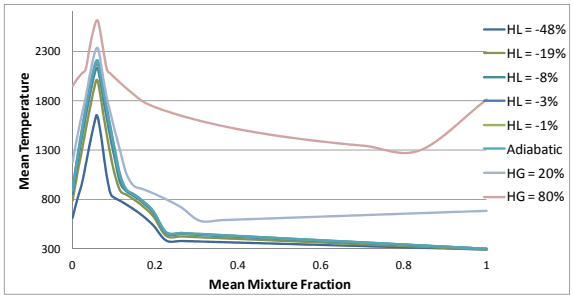

Figure 3: Tabulated temperature based on mixture fraction and scaled heat loss-gain.

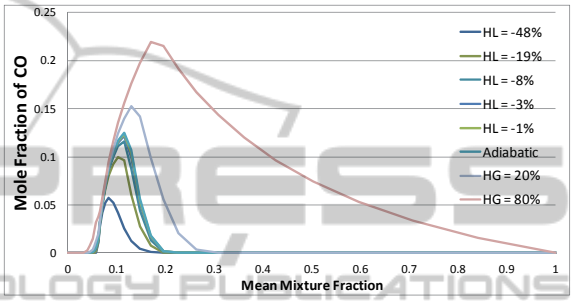

Figure 4: Tabulated CO mole fraction based on mixture fraction and scaled heat loss-gain.

3 INFLUENCE OF SWIRL NUMBER

In this section the flames for swirl numbers 0.14 and 0.74 are presented. Figure 5 depicts the mean mixture fraction, as well as the volumes of null axial velocity. Since the recirculation zones are composed by negative values of axial velocity, these isovolumes identify the boundaries of the recirculation zones. Swirl = 0.14 presents a large ORZ and lacks the IRZ. Whereas Swirl no. = 0.74 has a smaller ORZ and a central IRZ.

From the mixture fraction contours illustrated in Figures 5, it is clear the higher gradients of any variable are produced upwind of the IRZ. But for Swirl no. 0.14, the mixture fraction gradient is lower and the mixing region larger.

Figures 6 show the mixture fraction variance whose local maxima correspond with the region with high reaction rate. Swirl no. 0.14 has a larger reaction zone than that of swirl no. 0.74. It is clear the IRZ produces the blockage of the fuel jet, hence it is forced to be deflected and mixed with the annular jet. Also, the IRZ is mainly composed by products of reaction that keep thermal conditions adequate for ignition of the fresh mixture.

It is said that a flame with M shape tends to be instable, whereas a flame with V shape is more stable.

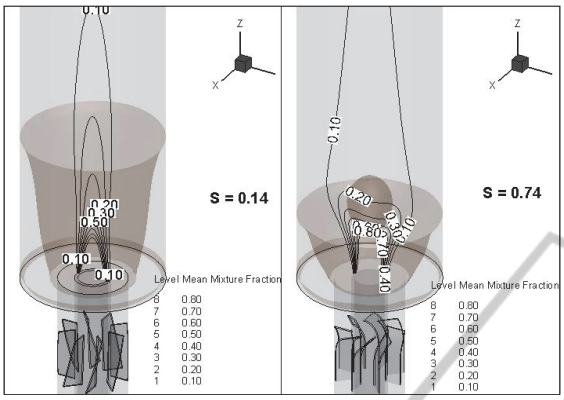

Figure 5: Longitudinal contours of Mean Mixture Fraction for different swirl numbers. Grey shadows are the iso-volume of null axial velocity.

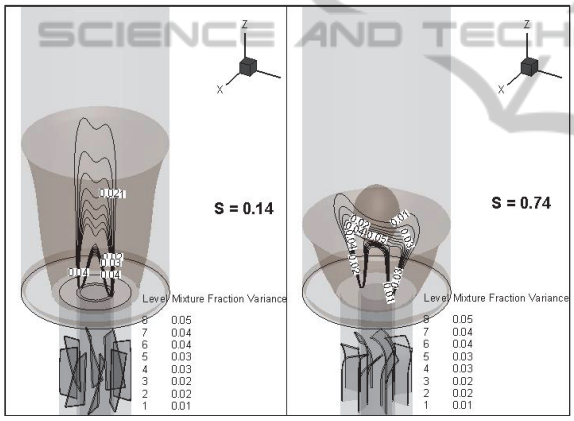

Figure 6: Longitudinal contours of Mean Fraction Variance. Grey shadows are the isovolume of null axial velocity.

Figures 7 present the radial profiles of axial velocity for non reactive and reactive cases and both swirl numbers: 0.14 and 0.74. Simulations without reactions are validated with the experimental results provided by Palm (Palm, 2006).

Reactive cases (RXN) produce higher axial velocities than non reactive cases (noRXN) because there is a reduction of density in the reaction products and there is mass conservation.

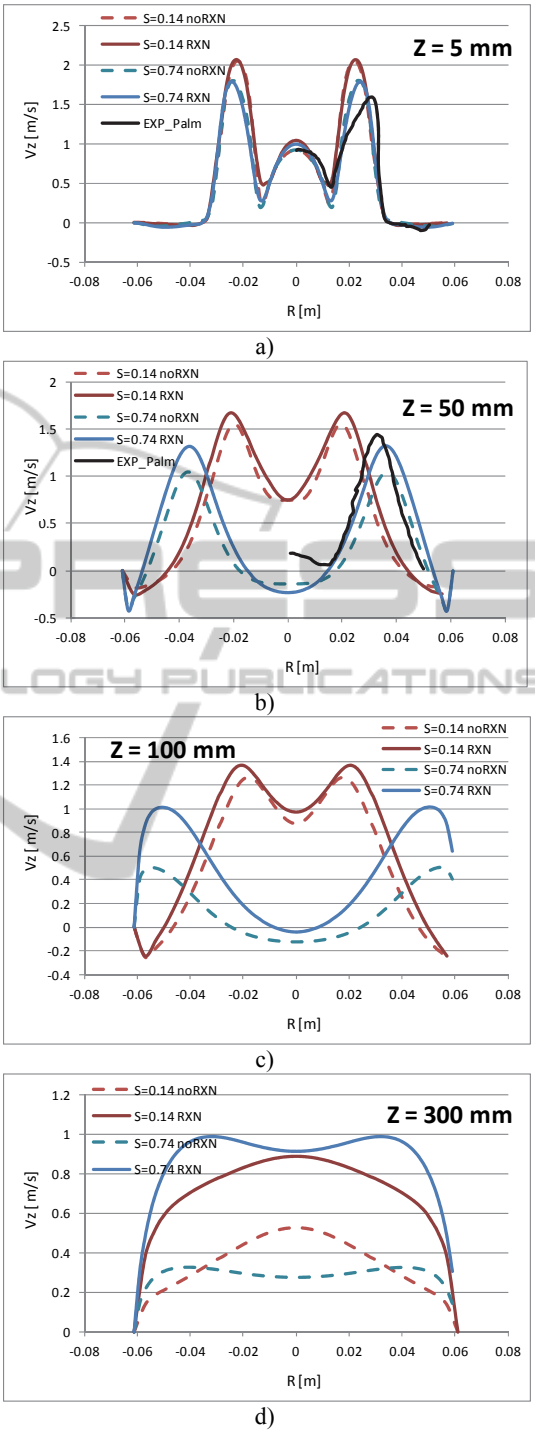

Figure 7: Radial profiles of axial velocities for different sections. a) Z = 5mm, b) Z = 50mm, c) Z = 100 mm and d) Z = 300 mm Experimental values from (Palm, 2006) for no reactive case.

Negative axial velocities in the periphery of the chamber are associated with the ORZ while these for radial position near zero are involved with the IRZ.

It is clear the IRZ is higher for no reactive case than for the reactive one for swirl 0.74.

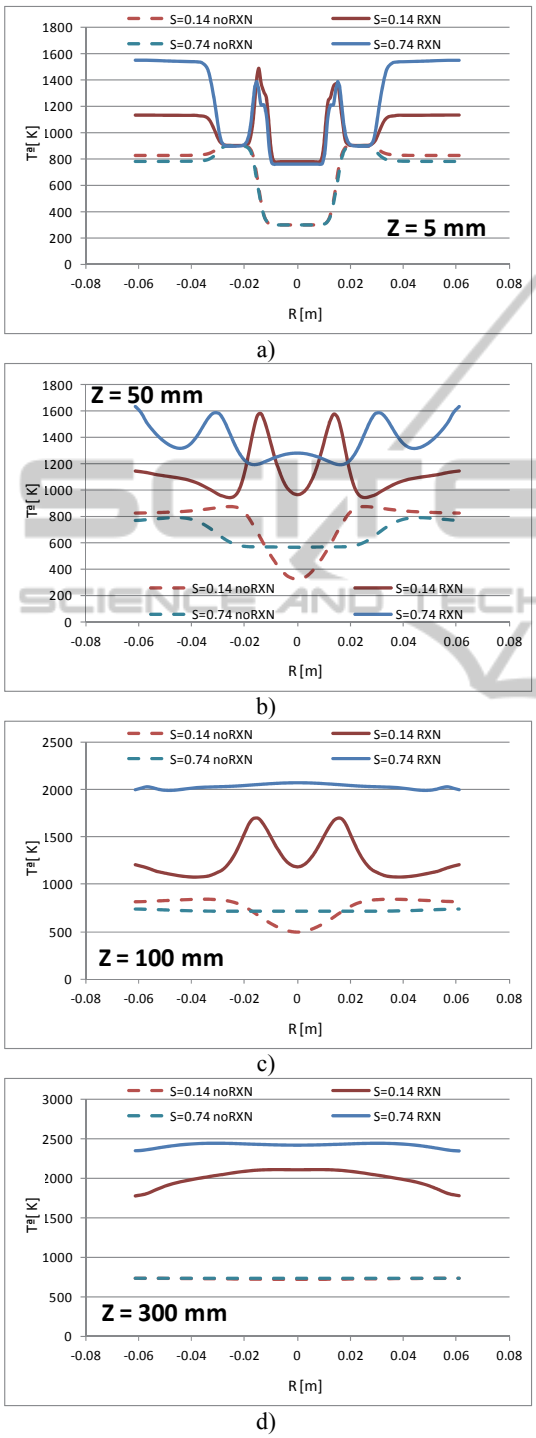

Figure 8: Radial profiles of temperature for different sections. a) Z = 5mm, b) Z = 50mm, c) Z = 100 mm and d) Z = 300 mm.

Figures 8 present the radial profiles of temperature for non reactive case to analyse the mixing, and reactive case.

For reactive cases, the maximum variance is observed for S=0.14, whereas for S=0.74 the flame is more compact in longitudinal direction with smaller difference of the local maxima. Hence, the flame is prone to instabilities with low Swirl numbers.

For reactive cases, the maximum variance is observed for S=0.14, whereas for S=0.74 the flame is more compact in longitudinal direction with smaller difference of the local maxima. Hence, the flame is prone to instabilities with low Swirl numbers.

4 CONCLUSIONS

Computational Fluid Dynamics has been used to study the interaction of two reactive confined coaxial jets. Annular swirling jet was generated with a swirl generator composed by 8 flat plates located in the annular nozzle. Averaged fluid field for no reactive case was validated with experimental results provided by Palm (Palm, 2006). Inner and outer recirculation zones where identified.

Low and high swirl injectors have been simulated and their pattern flow was contrasted. Numerical simulation uses PDF for combustion model and RNG k-ε turbulence model. These were found in this study to be suitable for turbulent swirl dominated flows.

Low swirling injectors does not promote the fluid to turn over near the centre of the chamber, resulting larger mixing zones with weak gradients of temperature and species' mass fractions.

Large swirling flows promote the formation of a vortex bulb near the axis of the chamber. The presence of the IRZ is a precursor of a smaller ORZ.

The lead stagnation point of the inner recirculation zone is responsible of deflecting the flame front and increases the mixing upstream of its lead stagnation point.

ACKNOWLEDGEMENTS

The author thankfully acknowledges the Spanish Ministry of Science and Innovation for the financial resources in the framework of the project reference ENE2011-25468.

We acknowledge PRACE for awarding us access to resource Curie-GENCI@CEA based in France and MareNostrum@BSC based in Spain. Ref. 2010PA1766

REFERENCES

García-Villalba M., Fröhlich J. and Rodi W. 2006_a Identification and analysis of coherent structures in the near field of a turbulent unconfined annular swirling jet using large eddy simulation- *Physics of Fluids (1994-present)* 18:5, 055103

García-Villalba M., and Fröhlich J. 2006_b. LES of a free annular swirling jet–Dependence of coherent structures on a pilot jet and the level of swirl. *International journal of heat and fluid flow 27:5, 911-923*

Jones W., Whitelaw J., 1982. Calculation Methods for Reacting Turbulent Flows: A Review. *Combustion and Flame* vol. 48 pp1-26.

Palm R., Grundmann S., Weismuller M., Saric S., Jakirlic S., Tropea C., 2006. Experimental characterization and modelling of inflow conditions for a gas turbine swirl combustor. *International Journal of Heat and Fluid Flow* 27 924–936.

Parra T., Vuorinen V., Perez R., Szasz R. and Castro F. 2014. Aerodynamic characterization of isothermal swirling flows in combustors. *International Journal of Energy and Environmental Engineering* 5:85

Parra-Santos M. T., Mendoza-Garcia V., Szasz R. Z., Gutkowski A. N., Castro-Ruiz F. 2015. Influence of swirling on the aero-thermodynamic behaviour of flames. *Combustion Explosion and Shock Waves Accepted for publication on 23/5/14.*

Kuo K., 1986. *Principles of Combustion*. John Wiley and Sons.

Roback R., Johnson B.V. 1983. Mass and momentum turbulent transport experiments with confined swirling coaxial jets, *NASA CR*-168252

Versteeg H. K., Malalasekera W. 1995. *Computational Fluid Dynamics, The finite volume method.*